Journal of Visualization, Vol. 12, No. 3 (2009) 251-258

Regular Paper

Experimental and Numerical Visualizations of Condensation Process in a Supersonic Ejector

Marynowski, T.*[1], Desevaux, P.*[2] and Mercadier, Y.*[1]

*1 Département de Génie Mécanique, Université de Sherbrooke, Sherbrooke, QC, J1K2R1, Canada.
*2 FEMTO-ST-UMR 6174, Dépt CREST, Université de Franche-Comté, Belfort F-90000, France
E-mail: philippe.desevaux@univ-fcomte.fr

Received 6 March 2008
Revised 13 November 2008

Abstract : The present study deals with the visualization of the droplet condensation phenomenon that can occur in ejectors powered by moist air. The condensation process is visualized through a numerical model of non-equilibrium condensation in high speed flows implemented by the present authors in a CFD code. The evolution of the region of condensation in the ejector with the primary stagnation pressure is examined both in the case without secondary flows and in the case with free entrainment of induced air. Laser tomography visualization is used to validate the computational results. The effects of some parameters such as the primary stagnation pressure and the humidity ratio in the primary and secondary air flows are also examined. Limitations of the present numerical model are discussed.

Keywords : Ejector, Supersonic flow, Condensation, Moist air, CFD, Laser tomography

1. Introduction

Ejectors are supersonic jet devices which take advantage of the entrainment effect caused by a motive supersonic jet to generate a suction force. This suction force may be used to create vacuum and/or to draw a secondary or induced flow. Ejectors are employed in many industries (Riffat et al., 2005), including chemical process and aeronautical industries, to compress, aspirate and mix fluids. The supersonic jets encountered inside ejectors may be accompanied, in more or less proportion, by condensation and evaporation processes within the primary and secondary flows. These phase changes are directly related to the supersonic flow properties and affect the flow characteristics due to the latent heat of the condensable fluid.

The condensation process in high speed flows has been studied for many years, especially in Laval nozzle (Kotake and Glass, 1981) and Ludwieg tube (Luo et al., 2007) flows. However, significant uncertainties remain about the mechanisms of formation and growth of droplets that render very complex the modeling of flows with condensation. Regarding the literature on ejectors, numerical studies of flows with condensation in these devices are very few or yielded no reliable results. However, qualitative studies (Desevaux, 2001) detailed the mechanisms of formation of droplets in moist air powered ejectors and have shown that water droplets may be produced by the supersonic expansion of the moist air flow in the primary nozzle or/and by the mixing between the supersonic primary jet and the induced moist air flow.

The work presented here deals with the development of a CFD model capable of taking into account the processes of condensation and evaporation in moist air powered ejectors (Marynowski, 2007). The numerical approach is realized with the Computational Fluid Dynamics (CFD) software FLUENT in which a 2D axisymmetric model of non-equilibrium condensation in high

speed flows was implemented. The model is based on that previously developed by the present authors to simulate incondensable flows in ejectors (Desevaux et al, 2001 ; Desevaux et al., 2004 ; Marynowski et al., 2006). The first stage of the overall study is presented here and focuses on the flow visualization of the condensation process in a supersonic ejector. Flow visualizations of the region of condensation obtained numerically are compared with laser tomography images of the condensation zone. The effects of some parameters such as the primary stagnation pressure and the humidity ratio in the primary and secondary air flows are also examined.

2. Experimental Procedure

A schematic view of the ejector configuration and of the flow visualization system used in this work is given in Figure 1. High-pressure moist air (mass flow rate m_1, absolute stagnation pressure P_1, humidity ratio g_1) enters the ejector to be accelerated to a supersonic speed through the primary Laval nozzle. By an entrainment-induced effect (viscous dragging and negative pressure), the secondary air (mass flow rate m_2, absolute stagnation pressure P_2, humidity ratio g_2) is sucked and accelerated into the secondary nozzle. Mixing and recompression of the resulting stream then occur, especially along the constant-area mixing chamber of the ejector. The primary/induced air mixture is finally discharged into the surrounding atmosphere at a pressure P_a. The ejector has a throat-area ratio $(D/d^*)^2 = 9$ and the primary nozzle is expected to produce a supersonic flow with an exit Mach number $M_1 = 2.3$. The ejector can operate with induced flows (free entrainment condition) or without secondary flows (vacuum operation).

Flow visualization is carried out by laser sheet illumination methods. The optical arrangement (Figure 1) uses a continuous wave argon laser (power of about 1 W at 488 nm) emitting a vertically polarized laser beam. An oscillating mirror generates a dynamic light sheet with a constant width slightly smaller than the mixing chamber diameter reflected in the upstream direction along the ejector axis. The observation direction is perpendicular to the flow axis (the secondary nozzle is made of transparent material). The process and the region of the condensation are visualized thanks to the light scattered by water droplets generated from the condensation of moisture in the primary and secondary flows. A previous study of the light scattered by these droplets (Desevaux, 2001) showed that they have an average diameter less than 0.1 μm.

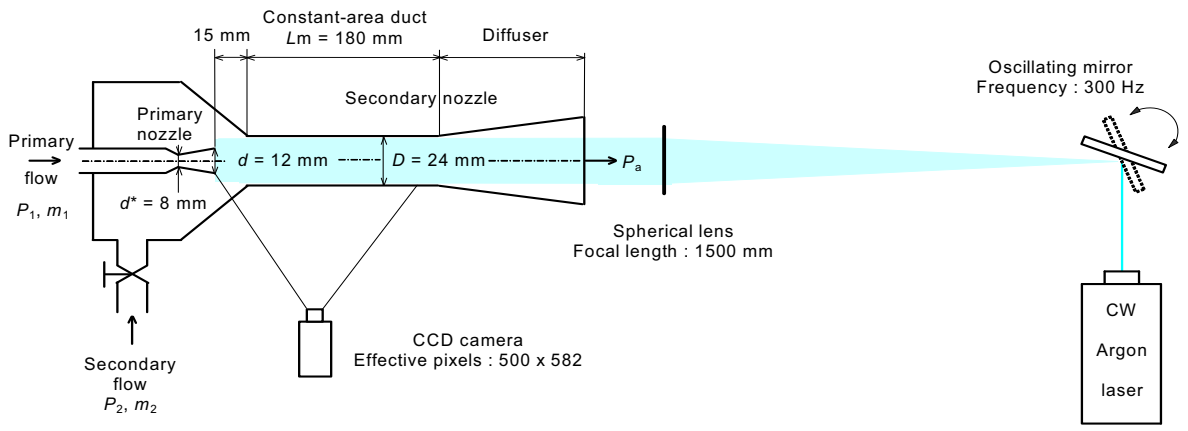

Fig. 1. Experimental setup

3. CFD model

The flow in the ejector is modeled using the commercial CFD package Fluent. The configuration of the ejector allows the 2D axisymmetric simulation of the flow. To minimize the computational requirement, only a half section of the ejector is simulated and symmetry conditions are assumed along the centreline as shown in Figure 2. A hybrid computational mesh (quadrilateral elements for the primary nozzle and the mixing chamber and triangular elements for the computational domain defined by the convergent part of the secondary nozzle) is used. Successive adaptations of the mesh have been performed to capture shock waves accurately and to obtain grid independent solutions for

a refined grid of approximately 50000 cells. The gas flow is a mixture of air and water vapour. The fundamental transport equations of mass, momentum and energy are solved sequentially for a steady-state solution using the segregated solver. Convective terms are discretized with a flux splitting method in order to capture shock accurately (second order upwind), while the diffusive terms use a central difference discretization. Turbulence is modeled using the standard k-ε model which has been found to simulate adequately flow phenomena in dry air powered ejectors (Marynowski et al., 2006 ; Desevaux et al. 2006).

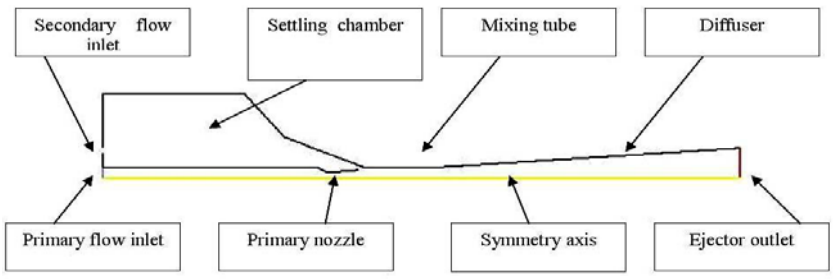

Fig. 2. Computational domain

The condensation modeling developed in this work (Marynowski, 2007) is based on the previous studies of Abraham (1974), Luitjen et al. (1999) and Lamanna (2000). The nucleation process is assumed to be homogeneous in nature and to follow the Classical Nucleation Theory (CNT). For the droplet growth, the Hertz-Knudsen model (Hill, 1966) is applied. Furthermore, no slip velocity between the gas and the droplets is considered.

Regarding the numerical convergence, a calculation is considered converged when the mass, momentum, energy and turbulence equations are balanced (i.e. when residues are stable and below 10^{-5}), when the total mass flow difference between inlets and outlet is less than 0.01% and also, for simulation with free entrainment, when the induced mass flow rate reaches a stable value.

Concerning the boundary conditions, a stagnation pressure is imposed at the inlet section of the primary nozzle, and the pressure at the outlet section of the ejector is fixed to the atmospheric pressure. Regarding the secondary flow inlet, a pressure inlet condition equal to the atmospheric pressure is imposed at a coaxial annular section equivalent to the real test section. For numerical simulations without entrainment of induced air, the secondary flow inlet is replaced by a wall boundary condition. A turbulence intensity of 5% is fixed at both inlet sections. For the humidity conditions, the use of a homogeneous nucleation model imposes an identical humidity condition at the primary and secondary inlets.

4. Results and Discussion

4.1 Evolution of the condensation zone with the primary stagnation pressure

The numerical/experimental comparison carried out in this study is purely qualitative (i.e. visual) and is based on visualizations of the flow in the mixing tube of the ejector. Figure 3 presents a typical set of flow visualizations obtained numerically and experimentally for the same flow conditions. This figure compares :

- the computational Mach number distribution in the mixing tube of the ejector (Figure 3a),
- the laser tomography image of the flow (Figure 3b),
- the condensate mass fraction distribution obtained by CFD (Figure 3c).

At first examination, we can note a good qualitative overall agreement between the different results. The visualization of the Mach number distribution and the le laser tomography image show a good concordance concerning the number and the location of the oblique shocks. For the region of condensation, CFD and experimental visualizations are also in relatively good agreement although the CFD model seems to predict condensation zone shorter than experiments.

Figure 3d gives the detail of the condensate mass fraction distribution in the primary nozzle. It clearly appears that the condensation occurs just downstream of the nozzle throat. The region of

condensation extends along the mixing tube and it may be seen in figures 2b and 2c that the water droplets are evaporated just before entering the ejector diffuser

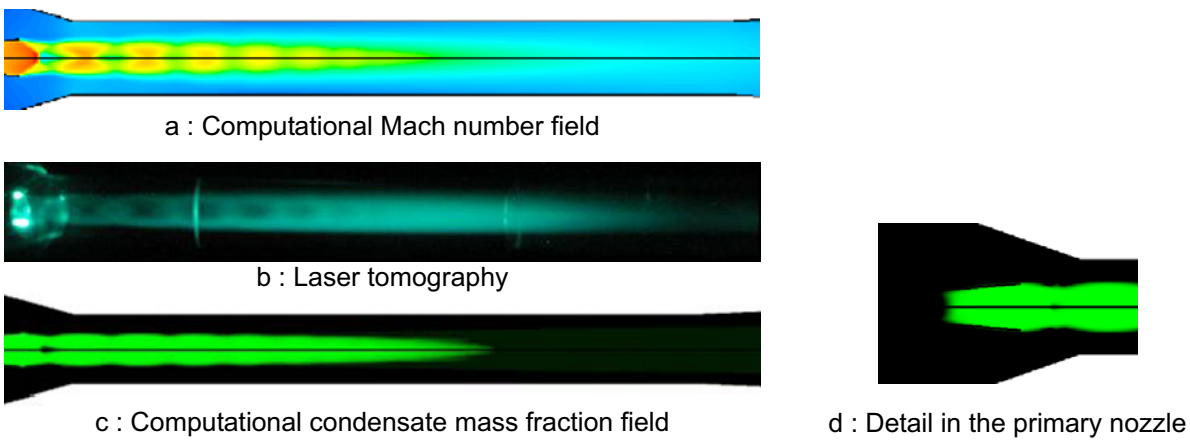

Fig. 3. Typical set of flow visualizations in the ejector mixing tube
(P_1/Pa = 3.75 ; Free entrainment condition ; g_{max} = 2.8 g of water/kg of dry air)

The series of images presented in Figures 4 and 5 compare experimental flow visualizations (top images) with computational visualizations of the condensate mass fraction distribution (bottom images). All the visualizations shown in these figures extend along about 180 mm from the primary nozzle exit (the flow is from left to right). Experimental visualizations are achieved by laser sheet illumination methods. The regions, which appear in bright green colour in the laser tomography images, correspond to the regions marked by scattering particles. These particles are fine water micro-droplets produced by condensation within the flow. A previous study (Desevaux, 2001) detailed the mechanisms of formation of these droplets and showed that the average diameter of these droplets does not exceed 0.1 μm.

Figure 4 presents the evolution and the extension of the condensation zone with the increasing primary stagnation pressure P_1 for free entrainment operating mode of the ejector. The condensate mass fraction distributions shown in this figure are obtained by fixing the same humidity condition at the primary and secondary inlets (i.e. g_{max} = 2.8 g of water/kg of dry air). The flow visualizations show the good agreement between the CFD predictions and the experimental results concerning the development of the condensation zone. However, the condensation zone appears slightly longer in the experimental flow visualization. This difference may be attributed to the presence, during the experiments, of substrates (i.e. suspended dust particles) which may stimulate the nucleation process and consequently increase the formation of water droplets within the flow. The presence of these eventual substrates is not taken into account by the homogenous model of nucleation used in the simulations. In the numerical flow visualizations corresponding to low values of pressure P_1, we can note the presence of dark zones located on the ejector axis just downstream the exit section of the primary nozzle. These flow regions without condensation (the condensate mass fraction is equal to zero in these zones) reveal that the whole of the water droplets produced in the primary nozzle are evaporated when they pass through the first oblique shock. The evaporation, which occurs through the following shocks, is also visible in the laser tomography images (succession of dark zones along the ejector axis). On the other hand, this evaporation is not visible in the numerical flow visualizations. It is because the CFD phase change model developed here is not sensitive enough to predict the evaporation of droplets passing through weak shocks.

Figure 5 is related to the ejector operating without induced flows. The experimental flow visualizations performed in these conditions show a weaker light scattering than those obtained with induced flows. This is due to the fact that the water droplets are here produced only by the supersonic expansion of the moist air through the primary nozzle and not by the mixing between the supersonic primary jet and the induced moist air flow. The condensation process is therefore weaker. Concerning the numerical results, images obtained without induced flow are comparable to those obtained with secondary flow, except for the length of the condensation zone. For this parameter, the

comparison between numerical and experimental visualizations is very satisfactory and better than for free entrainment conditions. This may be explained by the fact that when the ejector operates without induced flows, the absence of secondary flows reduces strongly the eventual presence of foreign particles (the primary air is filtered contrary to the secondary air which is directly sucked from the ambient atmosphere). The heterogeneous nucleation process, which is not taken into account in the present CFD model, is therefore limited during the experiments without induced flows. Furthermore, the process of condensation by mixing between the supersonic jet and the induced air flow is no more present when the ejector operates without induced flows. The experimental conditions are thus, in this case, closer to the numerical simulation conditions.

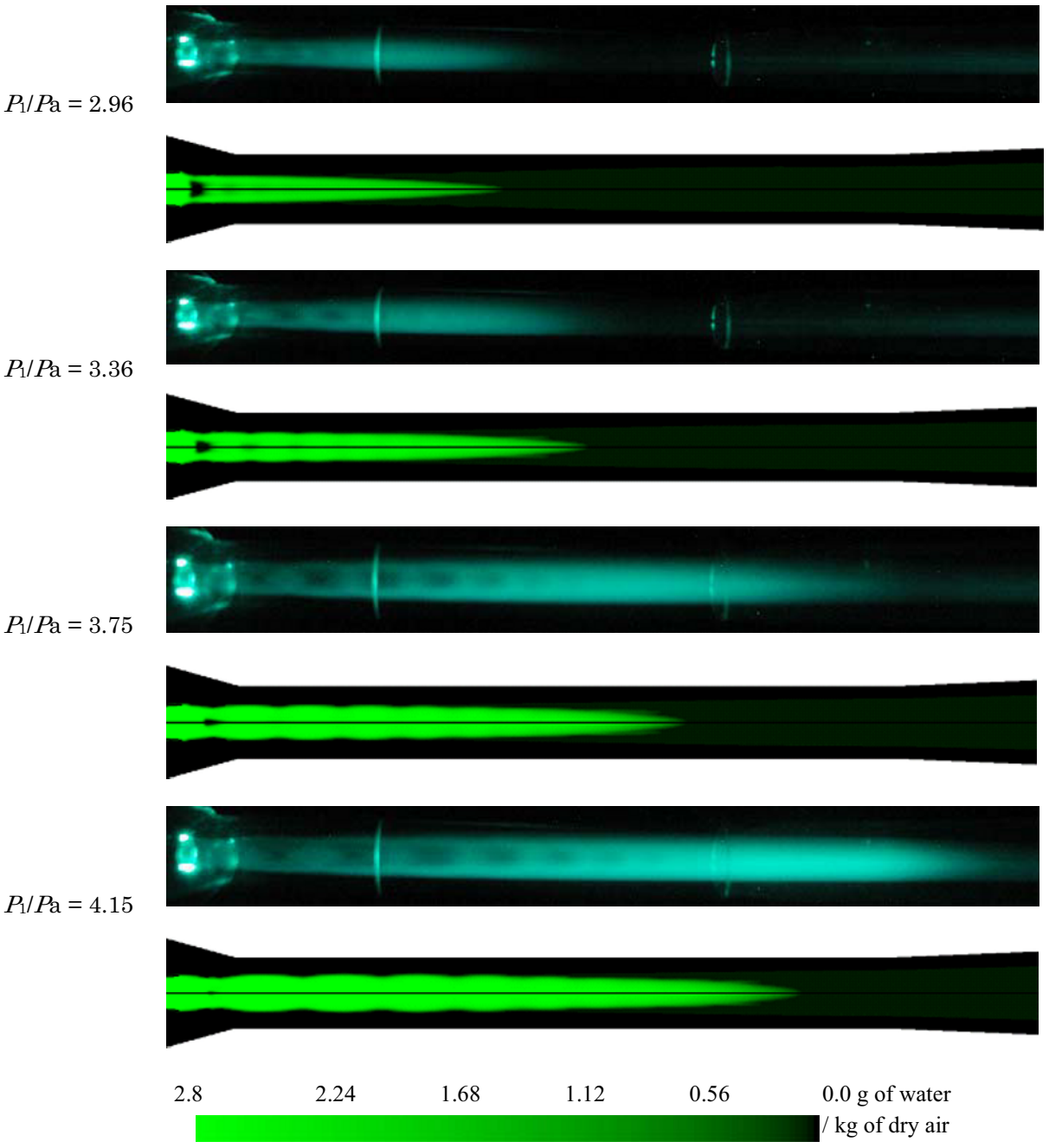

Fig. 4. Experimental and numerical flow visualizations of the condensation zone for different values of the primary pressure (Free entrainment operating mode)

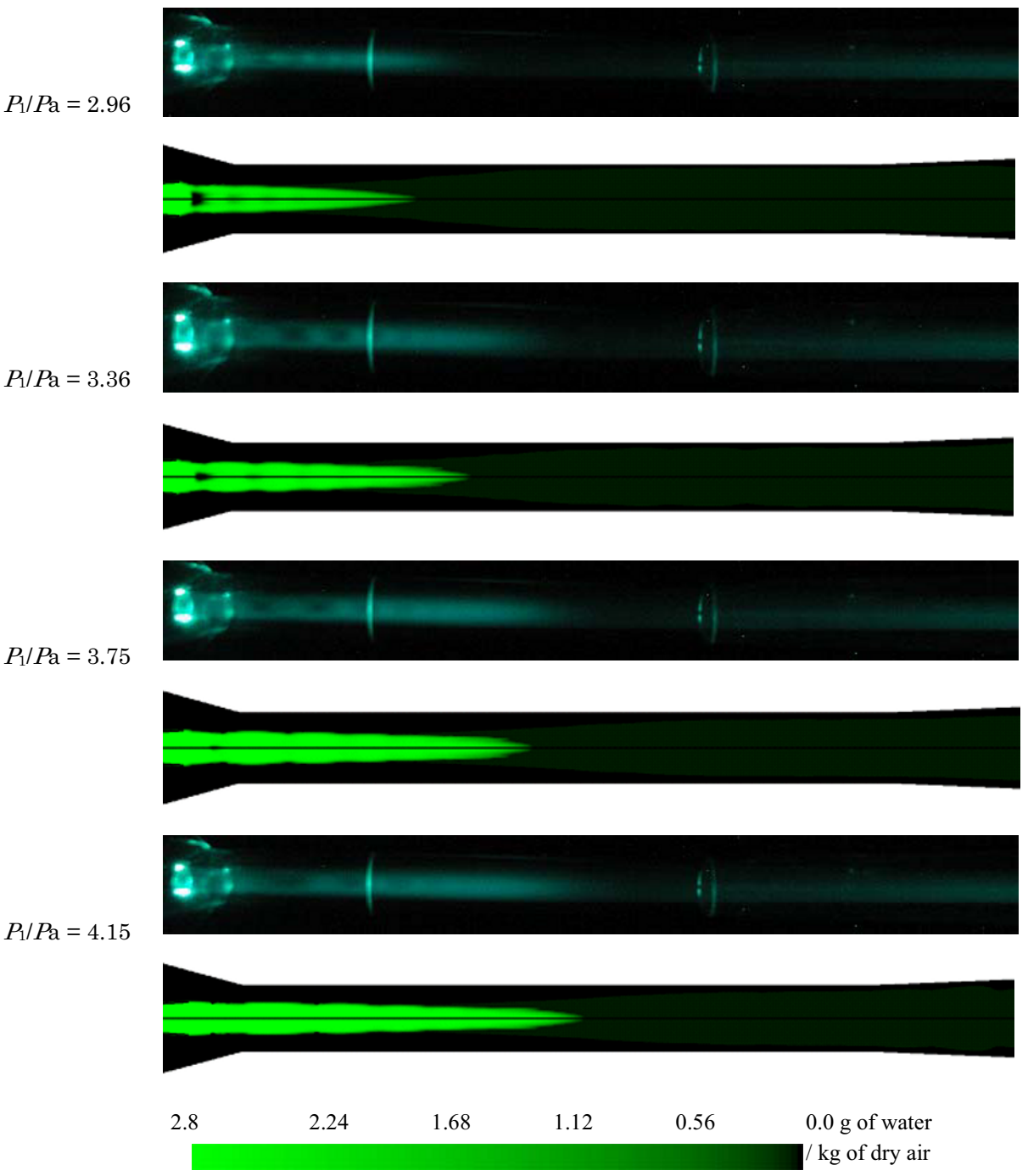

Fig. 5. Experimental and numerical flow visualizations of the condensation zone for different values of the primary pressure (Zero secondary flow operating mode)

4.1 Effect of the air inlet humidity ratio

The CFD model of flow with condensation is tested for several values of humidity ratio (comprise 2.8 to 6.0 g of water/kg of dry air) at the primary and secondary inlets. Figure 6 presents the evolution of the condensate mass fraction distribution as a function of the inlet humidity ratio. These numerical simulations are realized with free entrainment of secondary flows and for a fixed value of the pressure ratio P_1/P_a = 3.75. It may be noted that the CFD model predicts quite well the increase of condensation with increasing the inlet humidity ratio. Its effect is an extension of the zone of condensation accompanied by a slight extension of the shock train of the primary jet (Figure 7).
Although it is weakly pronounced, this extension of the supersonic jet with increasing the inlet humidity ratio is confirmed by the axial distributions of the Mach number plotted in figure 8. The

lengthening of the shock structure is accompanied by a significant augmentation of the maximum value of the flow Mach number. Thus, the flow Mach number does not exceed 2.35 when the ejector operates with dry air. The maximum value of Mach number passes through a value of 2.39 when the ejector is supplied with moist air with a humidity ratio of 2.8 g of water/kg of dry air, and reaches a value of 2.42 for an inlet humidity ratio of 6.0 g of water/kg of dry air. It seems to be confirmed that the condensation process, which takes place in the ejector, favours the development of the supersonic primary flow. The reason of this impact on the flow is not clear at the moment. This may be due to the change in the fluid properties and to the presence of the water droplets which probably reduce the velocity mismatch between primary and secondary flows (Al-Ansary, 2004).

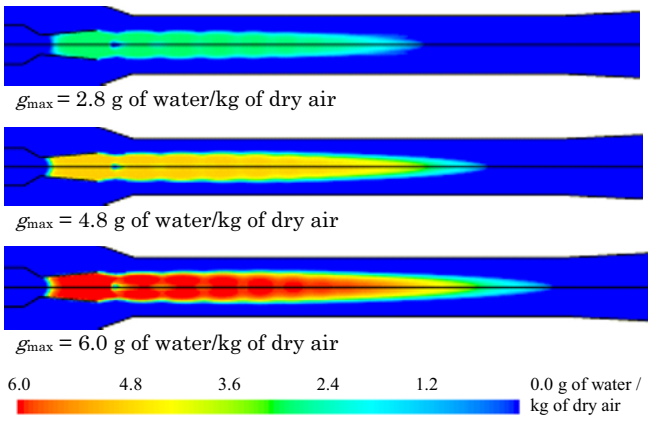

Fig. 6. Evolution of the condensate mass fraction distribution with increasing the inlet humidity ratio (Free entrainment condition ; P_1/Pa = 3.75)

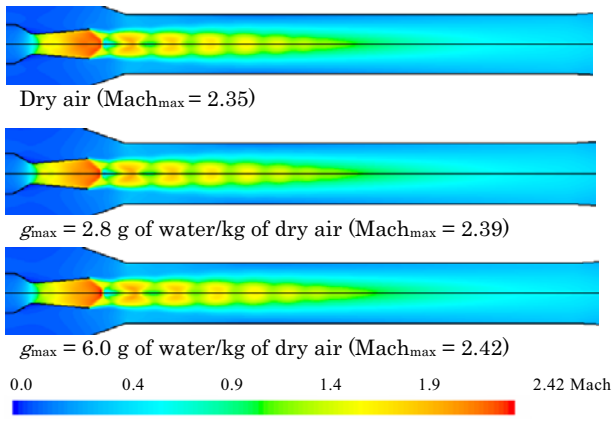

Fig. 7. Evolution of the Mach number distribution with increasing the inlet humidity ratio (Free entrainment condition ; P_1/Pa = 3.75)

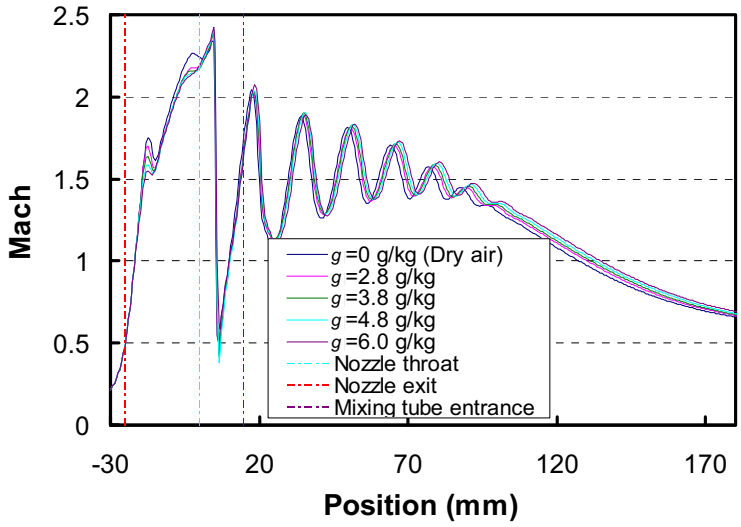

Fig. 8. Axial distributions of the Mach number for different inlet humidity conditions (Free entrainment condition ; P_1/Pa= 3.75)

4. Conclusion

This paper dealt with the visualization of the droplet condensation phenomenon in a moist air powered ejector. A CFD model capable of taking into account the processes of condensation and evaporation occurring in the ejector was developed and validated by means of laser sheet flow visualizations. Its capability to correctly predict the occurrence of the droplet condensation in the ejector for different operation modes was demonstrated. The first numerical results obtained were in good agreement with the experimental visualizations of the condensation zone. More quantitatively,

the CFD calculations showed that the local flow characteristics in the ejector are slightly affected by the condensation and evaporation processes. The eventual impact of these phenomena on the ejector performances (suction and entrainment capacities) should be investigated in more detail. Concerning the limitations of the present model, the following points must be noted :

- The CFD model permits actually the simulation of the flow in ejectors having the same humidity conditions at the primary and secondary inlets. In addition, this model is limited to low humidity rate (< 10%) and therefore cannot be applied to pure vapours.

- The model proposed here is based on the homogenous nucleation theory. It does not take into account the heterogeneous nucleation that occurs on foreign particles present in the ejector flow during the experiments and consequently tends to minimize the condensation process in the ejector. A heterogeneous nucleation model must be developed to model adequately the experimental conditions.

References

Abraham, F.F., Homogeneous Nucleation Theory, (1974), Academic Press, New York.

Al-Ansary, H.A.M. and Jeter, S.M., Numerical and experimental analysis of single-phase and two-phase flow in ejectors, HVAC &R Research, 10 (2004), 521-538.

Desevaux, P., Formation of nanodroplets in an air-induced ejector : a qualitative study by flow visualization, Can. J. Chem. Eng., 79 (2001), 273-278.

Desevaux, P., Lanzetta, F. and Bailly, Y., CFD modelling of shock train inside a supersonic ejector : validation against flow visualizations and pressure measurements in the case of zero-secondary flow, 10th International Symposium on Flow Visualization, F-0259, Kyoto, Japan (2002-8).

Desevaux, P., Mellal, A. and Alves de Sousa, Y., Visualization of secondary flow choking phenomena in a supersonic air ejector, Journal of Visualization, 7 (2004), 249-256.

Desevaux, P., Marynowski, T. and Khan, M., CFD prediction of supersonic ejectors performance, Int. J. Turbo and Jet Engines, 23 (2006), 173-181.

Hill, P.G., Condensation of water vapor during supersonic expansion in nozzles, J. Fluid Mech., 25 (1966), 593-620.

Kotake, S. and Glass, I.I., Flows with nucleation and condensation, Progress in Aerospace Sciences, 19 (1981), 129-196.

Lamanna, G., On nucleation and droplet growth in condensing nozzle flows, PhD Thesis, Technische Universiteit Eisndhoven, (2000).

Luitjen, C.C.M., Peeters, P. and Van Dongen, M.E.H., Nucleation at high pressure. II. Wave tube data and analysis, J. Chem. Phys., 111 (1999), 8535-8544.

Luo, X., Lamanna, G., Holten, A.P.C.and Van Dongen, M.E.H., Effects of homogeneous condensation in compressible flows : Ludwieg tube experiments and simulations, J. Fluid Mechanics, 572 (2007), 339-366.

Marynowski, T., Étude expérimentale et numérique d'écoulements supersoniques en éjecteur avec et sans condensation., PhD Thesis, (2007), University of Sherbrooke, Canada.

Marynowski, T., Mercadier, Y. and Desevaux, P., Characterization of geometric parameters impact on ejector performance, 13th International Heat Transfer Conference, Sydney, Australia, (2006-8).

Riffat, S.B., Jiang, L. and Gan, G., Recent development in ejector technology – A review, Int. J. Ambient Energy, 26 (2005), 13-26.

Author Profile

Tom Marynowski : He received his M.S. degree in Mechanical, Energy and Environmental Engineering in 2003 from University of Franche-Comté and his Ph.D in Mechanical Engineering in 2007 from University of Sherbrooke. His research interests are in the area of computational fluid dynamics, and more particularly, the modeling of internal supersonic flows with condensation.

Philippe Desevaux is an Assistant Professor at the University of Franche-Comté. He received a Ph.D. degree in Engineering Sciences from University of Franche-Comté in 1994. His research interests are in the field of fluid dynamics and include the use of CFD, the development of new investigation techniques and their application to aerodynamics, supersonic flows and two-phase flows.

Yves Mercadier is a Professor of Mechanical Engineering at the University of Sherbrooke. He received a Ph.D degree in engineering sciences from the National Polytechnic Institute of Grenoble in 1981. His research interests are in the area of thermal engineering, including flows with heat transfer and phase change.